Fast Contact Detection and Classification for Kinesthetic Teaching in Robots using only Embedded Sensors

Salt Ducaju, Julian; Olofsson, Björn; Robertsson, Anders; Johansson, Rolf

Published in:
Proc. 2022 31st IEEE International Conference on Robot and Human Interactive Communication (RO-MAN) Aug 29 - Sep 2, 2022

DOI:
10.1109/RO-MAN53752.2022.9900800

2022

Document Version:
Peer reviewed version (aka post-print)

Fast Contact Detection and Classification for Kinesthetic Teaching in Robots using only Embedded Sensors

Julian M. Salt Ducaju, Björn Olofsson, Anders Robertsson, Rolf Johansson

***Abstract*— Collaborative robots have been designed to perform tasks where human cooperation may occur. Additionally, undesired collisions can happen in the robot's environment. A contact classifier may be needed if robot trajectory recalculation is to be activated depending on the source of robot–environment contact. For this reason, we have evaluated a fast contact detection and classification method and we propose necessary modifications and extensions so that it is able to detect a contact in any direction and distinguish if it has been caused by voluntary human cooperation or by accidental collision with a static obstacle for kinesthetic teaching applications. Robot compliance control is used for trajectory following as an active strategy to ensure safety of the robot and its environment. Only sensor data that are conventionally available in commercial collaborative robots, such as joint-torque sensors and joint-position encoders/resolvers, are used in our method. Moreover, fast contact detection is ensured by using the frequency content of the estimated external forces, whereas external force direction and sense relative to the robot's motion is used to classify its source. Our method has been experimentally proven to be successful in a collaborative assembly task for a number of different experimentally recorded trajectories and with the intervention of different operators.**

I. INTRODUCTION

Physical Human–Robot Interaction (pHRI) has become a research topic of major interest during the later years in the robotics community [1]. The reason behind this is allowing robots to safely work in partially unknown environments where humans and robots can cooperate. One way that human operators can cooperate with the robot is through direct interaction, known as kinesthetic teaching [2], which is useful for robot trajectory reprogramming [3]. Consequently, collaborative robots have increased in popularity since their lightweight, compliant design is especially convenient when robots share their workspace with humans.

As part of the desire of increasing the flexibility and versatility of robots, it is common to find applications (*e.g.*, collaborative assembly [4]) where human cooperation is not the only contact that the robots may experience with their environment, and where unexpected collisions with obstacles may also occur. For this reason, it is essential that robots are capable of quickly distinguishing if a contact has occurred, and if so, whether it has been caused by human cooperation (defined as intentional) or by an obstacle collision (defined as accidental). Therefore, contact detection and classification, while the robot behaves in a compliant way with respect to its environment, is a key concern in these applications.

A. Previous Research

As summarized in [5], there are two main sets of methods, which are primarily based on external force/torque estimation, being used to detect and classify contacts: using machine-learning approaches [5]–[8], or analyzing their frequency content [9]–[11]. In such scenarios, a fast detection and classification is essential since a successful robot trajectory reprogramming should depend on it [2], [3], [12].

Machine-learning approaches have shown to provide promising results for contact detection and classification, but their fast execution may be challenging. In [6], the authors used the entire contact event to extract features that allow to discriminate between intended and unintended contacts. An extensive classification approach was presented in [7], but it cannot run in real-time. In [8], the authors were able to classify a detected contact in a minimum of 160 ms. Finally, an online classification method using machine learning was proposed in [5], but it is operator dependent and needs the joint load-torque signals of a previous, uncollided, execution of the trajectory.

In contrast, frequency-response analysis methods can achieve a faster detection and classification: in [9], the authors detected contacts in less than 50 ms, and the authors of [10], [11] detected and classified contacts in a single force direction in less than 10 ms. However, frequency-based methods come with their own challenges, one of the more significant being the difficulty of tuning their thresholds and cut-off frequencies. In [9], six different thresholding parameters per joint were needed to classify the contact situation based on filtered motor-current signals, which, unfortunately, are not available in some robot controller interfaces.

Moreover, these frequency-based contact-detection and classification methods are based on the premise that human voluntary cooperation with the robot presents forces with a lower rate of change than accidental collisions, and therefore, their frequency characteristics can be differentiated: cooperation will present lower frequency components than the accidental collisions. To sustain this assumption, the authors in [10] and [11] presented experimental data for one force direction recorded from an external force sensor mounted between the robot's flange and a handle.

B. Problem Formulation

In this paper, we address the problem of fast contact-detection and classification for kinesthetic teaching appli-

The authors are members of the ELLIIT Strategic Research Area at Lund University. This work was partially supported by the Wallenberg AI, Autonomous Systems and Software Program (WASP).

J. M. Salt Ducaju, julian.salt_ducaju@control.lth.se, B. Olofsson, A. Robertsson, and R. Johansson are with the Department of Automatic Control, LTH, Lund University, Lund, Sweden.

cations in collaborative robots relying only on available information provided by its embedded sensors, which in most cases are the joint motor encoders/resolvers that are able to provide joint angular positions (and joint angular velocity and possibly acceleration by differentiation), and the joint-torque sensors that are used to measure the joint applied torques. These variables are then used to estimate the external forces/torques applied to the robot. We refer to [13] for a summary of different methods to obtain these external forces/torques, and especially for the justification of the generalized momentum observer that was used in our experiments. Moreover, robot compliant control is used to ensure safety in a contact-rich environment and to allow human cooperation.

To solve the problem addressed in this paper, while ensuring fast contact detection, we evaluated the use of frequency-response analysis of the estimated external force and the benefits of comparing the robot Cartesian motion and its sensed external force. The method should allow a fast detection and to distinguish between human cooperation and accidental collisions in any contact direction for a collaborative assembly task using data only from robot embedded sensors. To evaluate this method, several experiments were performed, using the Panda robot by Franka Emika [14] with a peg-in-hole setup as seen in Fig. 2.

C. Outline

The paper is organized as follows: Sec. II presents the method for solving the problem described in Sec. I. Section III explains the experiments performed. Then, Sec. IV presents the results obtained. Finally, a discussion is included in Sec. V and conclusions are drawn in Sec. VI.

II. Method

First, we introduce the robot compliance controller used. Then, we evaluate the use of frequency-based contact detection and classification for our problem. Finally, we propose modifications and extensions to ensure contact detection in any direction and classification between human cooperation and obstacle collision for a collaborative assembly task.

A. Torque-Based Cartesian Impedance Control

External forces may be applied to the robot at any moment while executing a desired trajectory. Therefore, the robot must behave in a compliant way toward these forces to avoid any harm of both the robot and the colliding object. Also, a compliant robot behavior allows direct human cooperation without the need of switching to a dedicated admittance controller. The aim of a Cartesian impedance controller [15] is to establish a mass-damper-spring relationship between the Cartesian pose variation from its reference, $\Delta\xi$, and the Cartesian force, F [16]:

$$F = I\ddot{\xi} + B\dot{\xi} + K\Delta\xi \tag{1}$$

where I, B, and K are the virtual inertia, damping, and stiffness matrices, respectively. Further, $\Delta\xi = \begin{bmatrix}\Delta p^{\mathrm{T}} & \Delta\varepsilon^{\mathrm{T}}\end{bmatrix}^{\mathrm{T}}$, where the translation variations in the Cartesian pose are calculated with $\Delta p = p_d - \hat{p}$, and the rotation variations are calculated with $\Delta\mathcal{Q} = \hat{\mathcal{Q}}^{-1}\mathcal{Q}_d$, $\Delta\varepsilon$ being the vector part of the unit-quaternion representation of the rotation variation with respect to the base frame, $\Delta\mathcal{Q}$. Here, $\hat{\xi} = \begin{bmatrix}\hat{p}^{\mathrm{T}} & \hat{\mathcal{Q}}^{\mathrm{T}}\end{bmatrix}^{\mathrm{T}}$ is the estimated Cartesian pose of the robot end-effector computed from joint angle measurements, and $\xi_d = \begin{bmatrix}p_d^{\mathrm{T}} & \mathcal{Q}_d^{\mathrm{T}}\end{bmatrix}^{\mathrm{T}}$ is the reference Cartesian pose of the robot end-effector.

With F from Eq. (1), the task torque is calculated as:

$$\tau_{\text{task}} = J^{\mathrm{T}}(q)F \tag{2}$$

where $J(q)$ is the Jacobian relative to the base frame of the robot and q are the sensed joint angular positions. Finally, the contribution from Coriolis and centripetal forces, $C(q,\dot{q})$, is added to the task torque to obtain the reference torque:

$$\tau_{\text{ref}} = \tau_{\text{task}} + C(q,\dot{q})\dot{q} \tag{3}$$

where $\dot{q}$ represents the sensed joint angular velocities. The gravitational-forces term does not appear in Eq. (3) since the robot's internal controller takes care of the gravity compensation.

B. Frequency-Based Contact Detection and Classification

Previous research on frequency-based contact detection and classification is based on the idea that the frequency characteristics of motor currents or external force acting on the robot in an accidental collision situation are different from the ones obtained while a human is cooperating with the robot [9]–[11]. For a sliding time window, if the p–norm of the discrete Fourier transform of the force signal over a given frequency interval is greater than a user-defined force threshold, F_{th}, then it is considered that the contact should be classified an accidental obstacle collision [10], [11]. If not, then it is classified as interference from human cooperation.

Figure 1 illustrates the L_∞-norm of the frequency content of the force signal in the frequency range between $\omega_{\min}$ and $\omega_{\max}$ using a sliding window of N samples at every time step, as suggested in [10], but using the joint-torque sensors embedded in the robot to estimate the external force. This frequency range has an upper limit determined by the Nyquist frequency ($\omega_{\max} \leq 1/2h$) and a lower limit determined by the measurement duration ($\omega_{\min} \geq 1/Nh$), with h being the sample period. Moreover, the Cartesian impedance control parameters used are the same as in Sec. III-A.

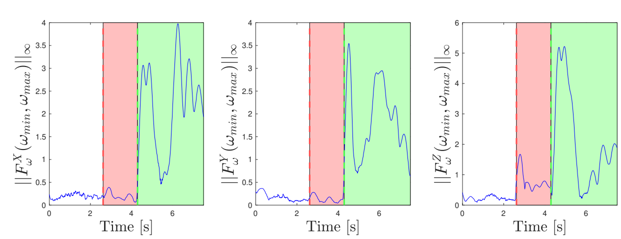

Fig. 1. Temporal evolution of the L_∞-norm of the frequency content for all three force directions: F^X, F^Y, and F^Z, in a collaborative assembly task (peg-in-hole). The frequency range used is $\omega \in [10, 100]$ Hz, and the temporal sliding window is $N = 500$ samples long.

In the trajectory used for Fig. 1, the robot transitions from free, undisturbed motion (white background), to obstacle collision (red background), and then to human cooperation (green background). The obstacle collision, which occurs along the Z-direction, can be distinguishable from the free motion when analyzing the frequency content that belongs to F_Z. However, human cooperation also causes an identifiable spike in this same force direction later in the trajectory. Therefore, when the experiments are performed for a robot with compliant behavior using the joint-torque sensors embedded in the robot instead of external force sensors, the distinction of frequency content between accidental collisions and cooperation becomes uncertain, which motivates the proposal of modifications and extensions to the method.

C. Contact Detection

From the analysis of Fig. 1, it can be concluded that force-thresholding can be useful for contact detection, but extra variables are needed for classifying the contact if only joint-torque sensors are used. Thus, our proposal consists of a decoupled process between contact detection and classification. For contact detection, the method presented in [10], [11] was extended to all three force directions. Therefore, the proposed detection process consists of evaluating if

$$\hat{F}^i_\omega > F_{\text{th}} \tag{4}$$

for $i \in \{X, Y, Z\}$, where F_{th} is the selected frequency-based threshold valid for any direction i for each time step, and $\hat{F}^i_\omega$ is equal to the L_∞-norm of the discrete Fourier transform of the external sensed force along direction i in the frequency range between $\omega_{\min}$ and $\omega_{\max}$ using a sliding window of N samples.

The contact-detection method, which is called at each time step, has been summarized in Algorithm 1. If the robot is moving in free motion (*STATE = FREE*), the condition (4) is evaluated in all directions (Algorithm 1, Line 2). If this condition is true, a contact is detected, and the classifier takes care of evaluating if the contact is accidental or if a human operator is collaborating with the robot (Algorithm 1, Line 5; detailed in Algorithm 2). The contact classifier uses the system's state at the exact time of the contact, which is obtained (in Algorithm 1, Line 4) by performing a backwards search in the external force signal from the contact-detection time along the contact's direction (determined in Algorithm 1, Line 3).

Moreover, while an accidental collision is occurring (*STATE = COLL*), an additional contact could be detected (whose source can be human cooperation) if the force threshold is violated again along any direction, with the exception of the directions that previously experienced the accidental collision (Algorithm 1, Line 9). The contact-detection algorithm will update the active collision directions if a collision along a new direction is detected or if the value of a previously collided direction has stopped violating the threshold (Algorithm 1, Line 13).

Furthermore, when a contact has been labelled as human cooperation (*STATE = COOP*), the contact-detection algorithm will only determine that the cooperation has stopped if the forces along all three directions are below the force threshold, F_{th} (Algorithm 1, Line 15).

Algorithm 1 Contact Detection

1: **if** STATE == FREE **then**
2: **if** Check contact == TRUE **then**
3: Get contact direction
4: Get contact time
5: STATE ← Contact Classifier (Algorithm 2)
6: **end if**
7: **else if** STATE == COLL **then**
8: Get contact direction
9: **if** Check new contact direction == TRUE **then**
10: Get contact time
11: STATE ← Contact Classifier (Algorithm 2)
12: **end if**
13: Update active collision directions
14: **else if** STATE == COOP **then**
15: **if** Check cooperation stopped == TRUE **then**
16: STATE ← FREE
17: **end if**
18: **end if**

D. Contact Classification

In contrast with contact detection, the frequency content of the estimated external force is not enough to classify the contact event when only using embedded sensors (as indicated in Fig. 1). Therefore, to properly categorize the contact in a kinesthetic teaching application, knowledge of the performed robot motion can be used.

Our classifier algorithm is based on two assumptions:

- **Assumption A1**: An accidental collision of the robot end-effector or attached tool with a static obstacle must occur in the direction of the movement and with the opposite sense from the one of the motion.
- **Assumption A2**: Human cooperation should have less dominant external force components in the direction of the robot's motion because of the typical spatial layout and interaction of a human operator and a robotic manipulator in kinesthetic teaching.

These two ideas are used to formulate an algorithm next, along with the explanation of the steps of the classifier algorithm.

The contact classifier will be activated once contact has been detected. The contact-classifying algorithm has been summarized in Algorithm 2. The first step is to analyze if, for any of the external forces sensed that have trespassed their threshold (where inequality (4) holds), the force is being applied in the same sense as the motion at the moment that this force signal started rising (Algorithm 2, Line 1). If this is the case, it is straightforward to affirm that human cooperation is occurring (*A1*):

$$\mathrm{sign}\left(\dot{\hat{F}}^{i}_{\mathrm{ext}}\dot{\hat{\xi}}^{i}\right) > 0 \tag{5}$$

only when $\hat{F}^{i}_{\omega} > F_{\mathrm{th}}$, $i \in \{X, Y, Z\}$, F_{th} being the selected frequency-based threshold, and $\dot{\hat{\xi}}$ being the time derivative of the estimated Cartesian pose of the robot end-effector. The time derivative of the estimated external force along direction i, $\dot{\hat{F}}^{i}_{\mathrm{ext}}$, is preferred compared to the estimated external force along direction i, $\hat{F}^{i}_{\mathrm{ext}}$, since the time step where this condition is evaluated is when the force signal starts rising.

The second step is, if the inequality (5) is not true for any of the detected contact directions, to perform a new test that evaluates the direction of the external force vector relative to the Cartesian velocity vector (Algorithm 2, Line 4). The reason for this is that compared to intuitive human cooperation for kinesthetic teaching, the largest external force components in accidental collisions must come from directions where the robot's velocity is the highest (*A2*):

$$||\vec{u}_{\dot{\hat{F}}_{\mathrm{ext}}} \oslash \vec{u}_{\dot{\hat{\xi}}}||_2 < \gamma \tag{6}$$

where $\vec{u}_j$ represents a unitary vector of variable j, γ is the threshold coefficient, and $||\cdot||_2$ is the L_2-norm. Also, $\oslash$ represents the Hadamard division: $C_{jk} = A_{jk}/B_{jk}$ if $C = A \oslash B$. The smaller the threshold coefficient γ is, the closer the external force will be when compared to the Cartesian velocity. If the inequality (6) is evaluated as true, the contact is classified as accidental collision.

Moreover, the inequality (6) is equivalent to evaluating if the unitary external force vector is contained in the ellipsoid defined by the robot's unitary Cartesian velocity vector:

$$\frac{x^2}{a^2} + \frac{y^2}{b^2} + \frac{z^2}{c^2} < 1 \tag{7}$$

where $[x, y, z] = \vec{u}_{\dot{\hat{F}}_{\mathrm{ext}}}$ and $[a, b, c] = \gamma\vec{u}_{\dot{\hat{\xi}}}$.

Furthermore, unitary vectors have been chosen to avoid having a dependence on the trajectory or on the applied force magnitude, since the classification should be trajectory-independent and also human-operator independent. Therefore, the algorithm only relies on the external force-vector direction with respect to the tangential direction of the motion.

Algorithm 2 Contact Classification

```
1: if A1 == TRUE then
2:     STATE ← COOP
3: else
4:     if A2 == TRUE then
5:         STATE ← COLL
6:     else
7:         STATE ← COOP
8:     end if
9: end if
```

III. Experiments

The goal of the experiments was to obtain realistic data of a collaborative assembly task where human operators were instructed to cooperate intuitively with the robot to evaluate the contact detection and classification method for kinesthetic teaching applications proposed in Sec. II.

A. Experimental Platform

The experiments were performed using the Panda robot by Franka Emika [14] mounted onto a table; the robot was able to record with a sample frequency of 1 kHz (sample period $h = 1$ ms), using the setup shown in Fig. 2. As mentioned earlier, we only used data from embedded sensors to estimate the variables of interest, $\hat{\xi}$ and $\hat{F}_{\mathrm{ext}}$, which were used for selecting and evaluating the threshold parameters for contact detection, F_{th}, and contact classification, γ. The end-effector Cartesian pose was obtained by applying forward kinematics, $\mathcal{K}$, to the joint angular-position readings provided by the joint encoders [17]:

$$\hat{\xi} = \mathcal{K}(q) \tag{8}$$

Moreover, the estimate of the external forces was obtained from the external joint-torques, which were estimated based on the generalized momentum observer for the Panda robot that was introduced in [13], by using the Jacobian relative to the base frame of the robot in an inverse way compared to the one presented in Eq. (2):

$$\hat{F}_{\mathrm{ext}} = J^{\dagger}(q)\hat{\tau}_{\mathrm{ext}} \tag{9}$$

where the superscript † denotes the Moore-Penrose pseudoinverse.

Furthermore, the Cartesian impedance control parameters (K, B, and I) of Eq. (1) were chosen to be as follows:

- The stiffness K was equal to 150 $[\mathrm{N/m}]$ for the translational degrees of freedom and equals to 10 $[\mathrm{N/rad}]$ for the rotational degrees of freedom.
- The damping B was equal to $2\sqrt{K}$.
- The inertia I was equal to 0.

The relationship between the Cartesian position variation and the task force will, with these parameters, behave along all degrees of freedom as a first-order system with a time constant equal to $2/\sqrt{K}$ [18]. This way, we ensured stability of the system and proper following of the trajectory reference (overdamped behavior).

B. Experimental Procedure

A cylinder insertion, or peg-in-hole, was the collaborative assembly task chosen for the experiments, as shown in Fig. 2. The reason for the selection of this task was that it presents a high amount of interaction with the environment: the hole where the piston must be inserted was narrow in comparison to the piston, and also the piston must make a vertical descent to avoid contacts. Therefore, the probability of an accidental collision was high if the reference trajectory was not accurate or if the controller introduced uncertainty in the motion. Furthermore, it is an application where the aid of a human

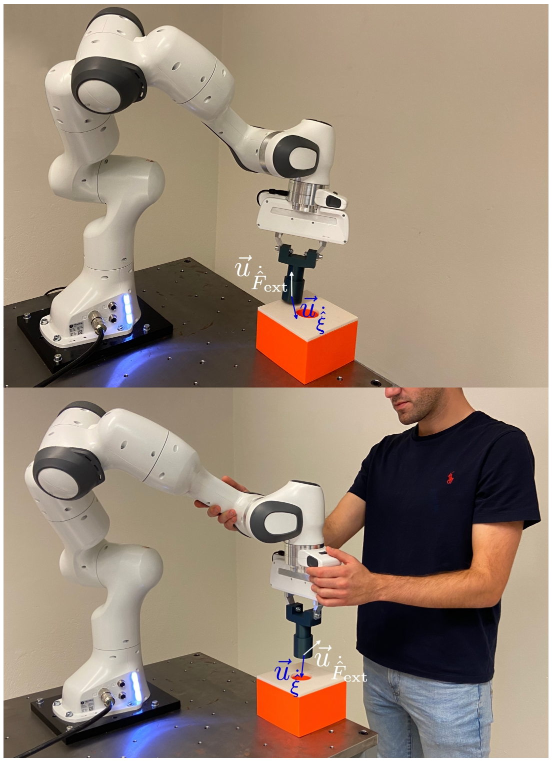

Fig. 2. Setup for the collaborative assembly task (peg-in-hole) used for the experiments. Figure 2-A (top) shows an accidental collision scenario, and Fig. 2-B (bottom) shows a human cooperation event. The unitary vector of external forces (white) and the unitary vector of Cartesian velocity (blue) were used in the contact-classification algorithm proposed in Sec. II-D. A video of the experiments can be found at [19].

operator can be valuable and it did not require a high level of skill for the operator.

The trajectories used range from almost-ideal trajectories, where the robot could complete the insertion task and the only collisions were with the borders of the hole of the box, to failed trajectories where the robot collided with the side of the box and the robot was not able to overcome this collision and insert the piston in the hole without human intervention. Other trajectories used were flawed with manifest collisions with the top of the box, and depending on the nature of the trajectory, the robot might be able to find its way to the hole with no human input. All trajectories were recorded several times using different initial poses to avoid a trajectory-dependent contact detection and classification.

The desired trajectory of Cartesian poses, $\xi_d(t)$, were recorded before the experiments by leading through the robot and recording the Cartesian pose of the robot end-effector. These trajectories served as the reference for the Cartesian impedance controller of Eq. (1). The reference trajectory was solely time-dependent and did not rely on the robot's current pose, since ideally, the contact-detection and classification algorithm should be implemented in a time-constrained scenario.

Additionally, regarding human cooperation, to test the validity of the assumptions proposed in Sec. II-D for a kinesthetic teaching application, the operators were instructed to cooperate in an intuitive manner with the robot to either help the robot with its cylinder insertion task or to push/pull the robot out of its trajectory to avoid colliding with the box. Moreover, since human cooperation in a kinesthetic teaching application may occur at different points of the trajectory in each of the runs, some of the human interventions occurred while the piston was in collision with the box and others while the robot was in free motion. Also, for the sake of data completeness, the operators were also instructed to vary the location of contact with the robot so that the human-cooperation events took place throughout all the links of the robot and not only at a location close to the robot end-effector.

Furthermore, as commented in previous research, human–robot cooperation may be very operator-dependent [5], [8], [9]. Therefore, a total of four different operators (including three external participants) individually manipulated the robot during the recording of the experiments to test the sensitivity and robustness of the classification. Also, the operators had different experience levels with robot manipulation to analyze the role of this variable for the contact-classification method proposed.

IV. Results

The total amount of data that were recorded included 266 contact events. These collision events were divided into 148 accidental obstacle collisions and 118 voluntary human cooperation events. In total, 28 accidental collisions and 28 human cooperation events (from a single human operator) were used for the parameter tuning, and the remaining contact events were used for the method's evaluation.

A. Tuning and Evaluation of the Method

First, for contact detection, the force threshold parameter has been assigned a value of $F_{\text{th}} = 0.85$ N, for all Cartesian directions. This value of the force-detection threshold allowed that all contacts recorded in the evaluation experiments were detected, and that no contact-detection false positive was detected. The frequency range used for detection was $\omega \in [10, 100]$ Hz.

Accidental collisions were detected within 71 ms on average, with a standard deviation of 31 ms. On the contrary, voluntary human-cooperation events were detected within 133 ms on average, with a standard deviation of 66 ms. Thus, the capacity of this method to detect contacts fast can be confirmed.

Additionally, the contact-classification threshold parameter was chosen to have a value of $\gamma = 6.2$. This value should be chosen conservatively high, since it is preferred to misclassify human cooperation events than accidental collisions. This idea will be further developed in Sec. V.

The results for the evaluation of the classification method are shown in Tables I and II. Table I displays the confusion matrix for all evaluation experiments performed. It can be seen how 93.3% of the accidental collisions were correctly classified (specificity), whereas for the cooperation events, 88.9% of them were correctly classified (sensitivity).

TABLE I

CONFUSION MATRIX FOR EVALUATION EXPERIMENTS

	Classified as	
	Collision	Cooperation
Collision	112 (93.3%)	8 (6.7%)
Cooperation	10 (11.1%)	80 (88.9%)

Moreover, Table II breaks down the recorded cooperation events of Table I into the four different operators involved in the evaluation experiments. As commented before, the success rate of the contact classifier varied depending on the human operator. For the method proposed, the sensitivity ranged from 85.2% to 96.2%. Therefore, the sensitivity achieved using this method was still high for the human operator with the lowest classification rate. Furthermore, the sensitivity of the method for experienced operators (Operators 1 and 2 in Table II) was on average 91% with a standard deviation of 5.3%, which is higher than the sensitivity of the method for inexperienced operators (Operators 3 and 4 in Table II), which was equal to 86.4% with a standard deviation of 1.2%.

TABLE II

DETAIL OF CONFUSION MATRIX FOR EACH HUMAN OPERATOR

	Cooperation classified as	
	Collision	Cooperation
Operator 1	1 (3.8%)	25 (96.2%)
Operator 2	3 (14.3%)	18 (85.7%)
Operator 3	4 (14.8%)	23 (85.2%)
Operator 4	2 (12.5%)	14 (87.5%)

B. *Contact Detection and Classification Example*

Figure 1 provides an example of the data extracted for one trajectory execution. The robot was initialized in free motion. It can be seen that at $t = 2.616$ s, a contact was detected along the Z-direction. The contact was detected 87 ms after the external force signal along the Z-direction starts rising. Once contact was detected, the contact-classifying part of the algorithm analyzed the force sense along the Z-direction and compared it to the motion component along this direction using condition (5). Since their signs were opposite, it cannot be determined that the contact was a human-cooperation event. Then, the inequality (6) was used. Since $||\vec{u}_{\dot{\hat{F}}_{\text{ext}}} \oslash \vec{u}_{\dot{\xi}}||_2 = 2.97 < 6.2 = \gamma$, it can be concluded that the contact was an accidental collision.

Moreover, at $t = 4.290$ s, a new contact was detected along the Y-direction just 85 ms after this new contact occurred. Now, by evaluating condition (5) at the contact time, it was seen that both the force component along the Y-direction and the motion along this direction share the same sign and therefore it is concluded that the contact belongs to the human cooperation category. Furthermore, if the inequality (6) had been evaluated in this situation, the contact would also have been labelled as a human cooperation, since $||\vec{u}_{\dot{\hat{F}}_{\text{ext}}} \oslash \vec{u}_{\dot{\xi}}||_2 = 41.84 > 6.2 = \gamma$.

Finally, no false positives occurred for contact detection for the entire trajectory shown in Fig. 1, since, for the accidental collision, no force violated the threshold along the X and Y-directions and no force violated the threshold along the Z-direction once the value was lower than this threshold. Also, for the human-cooperation segment, the force was at all times above the force threshold for some of the three Cartesian directions after $t = 4.290$ s.

V. DISCUSSION

In the event that only embedded sensors are available and the external force signal is estimated using the generalized momentum observer [13], which is currently implemented in commercial collaborative robots such as the Franka Emika Panda [14] and the KUKA LBR product family [20], the assumption, considered in [9]–[11], that the frequency content of the estimated force is easily distinguishable between voluntary human cooperation and accidental collisions with static obstacles is not certain anymore in a collaborative assembly task. However, we have experimentally demonstrated that the frequency content of the external force signal can still be used for contact detection in this application. Nevertheless, additional sensor information, provided by the embedded joint-position sensors, regarding the robot's motion prior to the detected contact, can be used to classify the contact.

Moreover, several aspects of the implementation of the proposed method allow freedom to the designer for their selection, and this also has several consequences. First, there is a trade-off between the contact-detection time, defined as the time between the contact occurs and when it is detected, and the force threshold parameter F_{th}: if shorter detection times are desired, more false positives in the contact detection will occur since F_{th} would be smaller. Using only embedded joint-torque sensors causes longer detection times when compared to previous research that included this same force threshold parameter but used external force/torque sensors for a single force-direction detection [10], [11]. Nevertheless, the force-threshold parameter value used in our experiments has been proven able to provide faster response times for all three force directions than alternative machine-learning methods [6]–[8], while presenting no false positives in contact detection.

Second, the contact classifier's threshold parameter, γ, can be varied depending on the desired ratio between the sensitivity (percentage of human cooperation events correctly classified) and the specificity (percentage of accidental collisions correctly classified), since it is not possible to obtain a threshold parameter that allows no ambiguity in the classifier part. Here, specificity must be prioritized to avoid false positives in human cooperation. This is because the proposed method is aimed to be used in a collaborative assembly task where the presence of accidental collisions is expected, and if human cooperation is detected, the cooperation event can be used for trajectory reprogramming using kinesthetic teaching [3].

Third, the method proposed solely requires tuning of two thresholding parameters (F_{th} and γ) to achieve a proper contact detection and classification along all three force directions, compared to the 6 parameters per joint used for tuning the method in [9] and to the single parameter needed in [10], [11] for a single force direction. Also, as discussed in [10], the choice of the virtual inertia, damping, and mass of Eq. (1) will have an effect on the sensed external force signal, and therefore, the two thresholding parameters used in our proposed method must be varied if the desired impedance behavior of the robot is different from the one described using the values defined in Sec. III-A.

The proposed method was not tested to detect transitions between accidental collision to free motion, or from cooperation to accidental collision since we were not interested in these situations in the experimental application used for evaluation. First, the peg-in-hole application would not have the accidental-collision to free-motion situation, since when the piston impacts the cylinder, it would not stop its impact without human intervention. Second, for this application, a human intervention for kinesthetic teaching would not end up in a purposeful direct transition to an obstacle collision. Also, the proposed method can detect human-cooperation events while an accidental collision with an obstacle is occurring, whereas this transition has not been tested by machine-learning methods [5]–[8] or by the previously-proposed frequency-based methods [9]–[11]. This feature is especially relevant for applications that use kinesthetic teaching for corrective trajectory demonstration [3].

In addition, the proposed method's accuracy (percentage of total contacts correctly classified) outperformed other methods previously presented (91.4% for the proposed method, 86.3% for the method in [5], 89.5% for the method in [7], and 81.9% for the method in [8]). The method presented in [6] provides the highest accuracy, 97.8%, but only one human operator was used for gathering experimental data. Also, the proposed method's accuracy (91.4%) was higher than the accuracy obtained when using the same relevant variables ($\vec{u}_{\dot{\hat{F}}_{\mathrm{ext}}}$ and $\vec{u}_{\dot{\xi}}$) as parameter estimates in Fisher's Linear Discriminant [21] for contact classification (83.3%).

Moreover, our method is novel compared to the methods in [5]–[8] in that it has been designed for kinesthetic teaching applications, where a human operator can lead-through the robot for trajectory reprogramming [3]: the robot's compliant behavior, contrary to the stiffer robot behavior in [5]–[8], allows lead-through without controller switching (as well as providing safety for both the robot and its environment), and also the method is able to classify a human-cooperation event happening while an accidental collision is occurring.

Furthermore, the proposed method, although its evaluation involved only four participants, can be considered robust with respect to different operators since the standard deviation between operators of the sensitivity was equal to 4.4 percentage points, which was lower than in other methods (10.1 percentage points in [5], where four operators were involved, and 7.3 percentage points in [8], where three operators were involved). Also, the difference in accuracy between trained and untrained operators was lower than in [8], being 4.6 percentage points (91% and 86.4%, respectively) the difference in our method compared to 14.6 percentage points (86.4% and 71.9%, respectively) in [8], which showed the validity of the assumptions for the intuitive human cooperation in kinesthetic teaching that were included in Sec. II-D for both trained and untrained operators in a collaborative assembly task. Thus, the proposed method can be used by different operators for kinesthetic teaching in these tasks without the need for retuning.

VI. Conclusion

Fast contact detection and classification based on the frequency-response analysis of the estimated external force signals was evaluated, and necessary modifications and extensions to detect and classify a contact in any direction for kinesthetic teaching applications were proposed. Cartesian impedance control was used to allow safe human cooperation. The only sensors used for obtaining the external force estimate were sensors that are conventionally embedded in commercial collaborative robots and whose values were easily attainable: joint-torque sensors and joint-position encoders/resolvers.

The proposed modified method was proven to provide accurate results for both accidental collision with stiff and static obstacles and voluntary human cooperation in a collaborative assembly task. In addition, the method is trajectory-independent, and was tested for a meaningful number of different operators, showing interesting results for both trained and untrained operators.

References

[1] V. Villani, F. Pini, F. Leali, and C. Secchi, "Survey on human–robot collaboration in industrial settings: Safety, intuitive interfaces and applications," *Mechatronics*, vol. 55, pp. 248–266, 2018.

[2] S. Wrede, C. Emmerich, R. Grünberg, A. Nordmann, A. Swadzba, and J. Steil, "A user study on kinesthetic teaching of redundant robots in task and configuration space," *Journal of Human-Robot Interaction*, vol. 2, no. 1, pp. 56–81, 2013.

[3] M. Karlsson, A. Robertsson, and R. Johansson, "Autonomous interpretation of demonstrations for modification of dynamical movement primitives," in *IEEE Int. Conf. on Robotics and Automation (ICRA)*, Singapore, 29 May–2 Jun. 2017, pp. 316–321.

[4] B. Sadrfaridpour and Y. Wang, "Collaborative assembly in hybrid manufacturing cells: An integrated framework for human–robot interaction," *IEEE Transactions on Automation Science and Engineering*, vol. 15, no. 3, pp. 1178–1192, 2018.

[5] G. Cioffi, S. Klose, and A. Wahrburg, "Data-efficient online classification of human-robot contact situations," in *European Control Conference (ECC)*. Saint Petersburg, Russia: IEEE, May 12–15, 2020, pp. 608–614.

[6] S. Golz, C. Osendorfer, and S. Haddadin, "Using tactile sensation for learning contact knowledge: Discriminate collision from physical interaction," in *IEEE Int. Conf. on Robotics and Automation (ICRA)*, Seattle, USA, May 26–30, 2015, pp. 3788–3794.

[7] D. Popov, A. Klimchik, and N. Mavridis, "Collision detection, localization & classification for industrial robots with joint torque sensors," in *26th IEEE Int. Symp. on Robot and Human Interactive Communication (RO-MAN)*, Lisbon, Portugal, Aug 28–31, 2017, pp. 838–843.

[8] N. Briquet-Kerestedjian, A. Wahrburg, M. Grossard, M. Makarov, and P. Rodriguez-Ayerbe, "Using neural networks for classifying human-robot contact situations," in *18th European Control Conference (ECC)*, Naples, Italy, Jul 25–28, 2019, pp. 3279–3285.

[9] M. Geravand, F. Flacco, and A. De Luca, "Human-robot physical interaction and collaboration using an industrial robot with a closed control architecture," in *IEEE Int. Conf. on Robotics and Automation (ICRA)*, Karlsruhe, Germany, May 6–10, 2013, pp. 4000–4007.

[10] A. Kouris, F. Dimeas, and N. Aspragathos, "Contact distinction in human-robot cooperation with admittance control," in *IEEE Int. Conf. on Systems, Man, and Cybernetics (SMC)*, Budapest, Hungary, Oct 9–12, 2016, pp. 1951–1956.

[11] ——, "A frequency domain approach for contact type distinction in human–robot collaboration," *IEEE Robotics and Automation Letters*, vol. 3, no. 2, pp. 720–727, 2018.

[12] S. Haddadin, A. Albu-Schäffer, A. De Luca, and G. Hirzinger, "Collision detection and reaction: A contribution to safe physical human-robot interaction," in *IEEE/RSJ Int. Conf. on Intelligent Robots and Systems (IROS)*, Nice, France, Sep 22–26, 2008, pp. 3356–3363.

[13] S. Haddadin, A. De Luca, and A. Albu-Schäffer, "Robot collisions: A survey on detection, isolation, and identification," *IEEE Transactions on Robotics*, vol. 33, no. 6, pp. 1292–1312, 2017.

[14] *Panda – Data Sheet*, Franka Emika, 2019.

[15] N. Hogan, "Impedance control: An approach to manipulation: Parts I–III," *J. Dynamic Syst., Measurement, and Control*, vol. 107, no. 1, pp. 1–24, 1985.

[16] A. Albu-Schäffer and G. Hirzinger, "Cartesian impedance control techniques for torque controlled light-weight robots," in *IEEE Int. Conf. on Robotics and Automation (ICRA)*, vol. 1, Washington DC, USA, May 11–15, 2002, pp. 657–663.

[17] P. Corke, *Robotics, Vision and Control: Fundamental Algorithms in MATLAB*, 1st ed. Springer, Berlin, Germany, 2013.

[18] D. A. Lawrence, "Impedance control stability properties in common implementations," in *IEEE Int. Conf. on Robotics and Automation (ICRA)*, Philadelphia, USA, Apr 24–29, 1988, pp. 1185–1190.

[19] "Experiments video," https://youtu.be/5Bq4oB6nDbw.

[20] R. Bischoff, J. Kurth, G. Schreiber, R. Koeppe, A. Albu-Schäffer, A. Beyer, O. Eiberger, S. Haddadin, A. Stemmer, G. Grunwald, and G. Hirzinger, "The KUKA-DLR lightweight robot arm—A new reference platform for robotics research and manufacturing," in *41st Int. Symp. on Robotics (ISR)*, Munich, Germany, Jun 7–9, 2010, pp. 1–8.

[21] R. A. Fisher, "The statistical utilization of multiple measurements," *Ann. Eugen.*, vol. 8, no. 4, pp. 376–386, 1938.